Sborník vědeckých prací Vysoké školy báňské - Technické univerzity Ostrava
číslo 3, rok 2009, ročník LII, řada hutnická,
článek č. 1541

Jiří KLIBER[1], Kamil DROZD[2], Tomáš KUBINA[3], Jaromír HORSINKA[4]

COMPUTATION OF HOT FORMING EFFICIENCY

VÝPOČET EFEKTIVITY DEFORMACE ZA TEPLA

[1] *Prof., Ing., CSc.; Faculty of Metallurgy and Materials Engineering VŠB-Technical University, Ostrava, CZ*
[2] *Ing.; Faculty of Metallurgy and Materials Engineering VŠB-Technical University, Ostrava, CZ*
[3] *Ing., Ph.D.; Faculty of Metallurgy and Materials Engineering VŠB-Technical University, Ostrava, CZ*
[4] *Ing.; Faculty of Metallurgy and Materials Engineering VŠB-Technical University, Ostrava, CZ*

Abstract

Processing maps on hot rolled 9 Cr steel have been developed in the range 800–1100 °C and 0,1–100 s^{-1} by plastometric hot plane strain compression test (PSCT) with a view to examine whether the hot workability is efficient. Briefly, the work-piece undergoing hot deformation is considered to be a dissipator of power and the strain rate sensitivity *m* of flow stress is the factor that partitions power between deformation heat and microstructural changes. The variation of efficiency of power dissipation with temperature and strain rate represents a power dissipation map which is generally viewed as an iso-efficiency contour map. Hot forming behaviour of stainless steel is characterised in processing maps developed on the basis of the Dynamic Materials Model. The material could exhibit a dynamic recrystallization domain in the temperature range of high than 1000 °C or higher and strain rate of 1 s^{-1}. Regarding efficiency, optimum hot workability (according to the range of testing) of energy dissipation occurs at 1200 °C. The assemblage of the processing map is described.

Abstrakt

Byly sestaveny procesní mapy za tepla tvářené 9 Cr oceli pro rozsahy teplot 800–1100 °C a rychlosti deformace od 0,1–100 s^{-1} · K tomu se využila plastometrická tlaková zkouška s rovinnou deformací (PSCT) s cílem sledovat účinnost procesu tváření za tepla. Lze konstatovat, že tvářený kus podléhající deformaci je disipátorem energie a koeficient rychlosti deformace *m* z křivky napětí-deformace je tím parametrem, který rozděluje sílu mezi vývin deformačního tepla a mikrostrukturní změny. Změny efektivity disipace s teplotou a rychlostí deformace představují disipační (výkonovou, procesní) mapu, kterou je možné zobrazit jako isočáry v ploše. Chování za tepla tvářené oceli je tedy charakterizováno dynamickým materiálovým modelem, ve kterém lze nalézt oblasti s probíhající dynamickou rekrystalizací, zde v oblasti teplot vyšších než 1000 °C a s rychlostmi deformace nad 1 s^{-1}. S ohledem na účinnost procesu a disipační energii (na základě rozsahu provedených zkoušek) se zde konkrétně jeví jako optimální oblast nad 1200 °C. V práci je popsáno vytvoření procesní mapy.

Key words: processing maps, plastometric hot plane strain compression test (PSCT), Dynamic Materials Model

1. Introduction

Existing experimental engineering enables to obtain accurate stress-strain curves for various thermomechanical parameters. Usually, torsion plasticity equipment is used for obtaining of the whole scope whose indisputable advantage is possibility of conduction of testing always at two same constant parameters – usually at one temperature and various strain rate, eventually at constant strain rate and various temperatures – while strain is a variable value. At assessment of 9 Cr types of steel, increased temperature results in shift of stress-strain peak to the left to the smaller strains and it is usual, that at temperatures of 1100 °C the strain value for initiation of dynamic recrystallization is on the limit of real removals in operation, i.e. around actual logarithmic strain of 0,3; which represents relative deformation about 35 %.

The purpose of the paper is to provide you with basic information on creation of technology map (Ashby plasticity maps are something else) which can be used for optimization of formability and later for checking microstructure. The output are graphs of effectiveness based on thermodynamic values, which reflect in the forming process in combination of all three basic thermomechanical parameters which result in the size of strain resistance, i.e. stress. Basically, the method involved is described in references [1-9]. According to [10] dynamic recovery of this steel occurs at lower forming temperatures while recovery caused by recrystallization was observed at higher temperatures even by strain rate.

Technological maps are based on the principle that the formed object is considered to be a dissipater of energy. The work-piece undergoing hot deformation is considered to be a dissipator of power and the strain rate sensitivity m of flow stress is the factor that partitions power between deformation heat and microstructural changes is given by

$$P = \int_0^{\dot{\varepsilon}} \sigma \cdot d\dot{\varepsilon} + \int_0^{\sigma} \dot{\varepsilon} \cdot d\sigma = G + J \qquad (1)$$

where σ is the flow stress in MPa and $\dot{\varepsilon}$ is the strain rate in s^{-1}. The first integral is called G content representing deformation heat and the second one a J co-content, which is a complementary part of G content, representing microstructural dissipation. At a given temperature of strain J value is determined as

$$J = \frac{m}{m+1} \sigma \dot{\varepsilon} \qquad (2)$$

The strain rate sensitivity m of flow stress is the factor that partitions power between deformation heat and microstructural changes since:

$$\frac{dJ}{dG} = \frac{\dot{\varepsilon} \cdot d\sigma}{\sigma \cdot d\dot{\varepsilon}} = \frac{\dot{\varepsilon} \cdot \sigma \cdot d \ln \sigma}{\sigma \cdot \dot{\varepsilon} \cdot d \log \dot{\varepsilon}} \approx \frac{\Delta \log \sigma}{\Delta \log \dot{\varepsilon}} = m \qquad (3)$$

J value, which is non-linear dissipation energy is unified through ideal dissipation at exponent of strain rate hardening ($m = 1$) and mutual relation is in fact effectiveness of energetic dissipation, or in other wording, it may represent effectiveness of engineering forming process.

$$\frac{\Delta J / \Delta P}{(\Delta J / \Delta P)_{linear}} = \frac{m/(m+1)}{1/2} = \frac{2m}{m+1} \equiv \eta \qquad (4)$$

Variable value of effectiveness η which is metaphorically depending on the temperature and strain rate, enables to set up technological maps. Should any changes occur in the material which cannot be described by conventional equations, for example for strain resistance or level of softening mainly due to non-monotonous situation then, the only areas shown, based on these technological maps, are the arisen areas enabling also control of microstructural changes.

2. Experiment

As the first steps at evaluation are concerned, and the key of this paper are two newly presented facts on course of effectiveness, we will limit ourselves to the statement that for set up of equations and tables of strain resistance older records of overall research of 9Cr steel pipes for energetics were used. For description of stress-strain curves were used perhaps today's standard methods consisting in calculation of activation energy Q and of other constants. Just for simplification of rather complicated equations and complete equation has been successively set up from experimental values for σ_{p-c} (sigma peak calculated in MPa):

$$\sigma_{p-c} = \arg\sinh\left[\frac{\dot{\varepsilon}\exp\left(\frac{Q}{RT}\right)}{A}\right]^{\frac{1}{n}} B\,\varepsilon^{d} \qquad (5)$$

while Q is apparent activation energy; T is temperature in K; A is constant; n is constant - reversed value of gradient in graphic dependence $\ln Z = \ln\left[\sinh(\alpha\sigma)\right]$; B is constant; ε is strain; $\dot{\varepsilon}$ is strain rate in s^{-1}; d is exponent of strain hardening.

More detailed comparison showed minor shortcomings of this equation, we returned firstly to previously verified form [11]

$$\sigma_{p-c} = \arg\sinh\left[\frac{\dot{\varepsilon}\exp\left(\frac{Q}{RT}\right)}{A}\ln\left(1+\varepsilon\right)^{1+b}\right]^{\frac{1}{n}} B\,\varepsilon^{d} \qquad (6)$$

which better describes experimental values. Trials and successive elimination of the member ε^{d} in the equation (5) can be also considered possible. Due to simplicity and regarding the shape of curves which do not exhibit dramatic drop, so called complete equation in the form [12-14] was not selected, but the simple form in shape of as Eq.(7) was used

$$\sigma_{p-c} = \frac{1}{\alpha}\arg\sinh\left[\frac{\dot{\varepsilon}\exp\left(\frac{Q}{RT}\right)}{A}\right]^{\frac{1}{n}} \qquad (7)$$

where A=$1{,}21 \cdot 10^{16}$; Q=506 045 J/mol; T is temperature in K (here in range of 1073-1533); α=0,029335. The strain peak value calculated ε_{p-c} were acquired from two separate calculations initially according Eq. (8), or afterwards using Eq. (9), once more for simplicity and more accurately conformity Eq. (8) was employed of final equation (10)

$$\varepsilon_{p-c} = \dot{\varepsilon}^{k} \exp\left[\arg\sinh\left(Y + \frac{X}{T}\right)\right] \tag{8}$$

$$\varepsilon_{p-c} = A\,\dot{\varepsilon}^{k} \exp\left(\frac{KQ}{RT}\right) \tag{9}$$

$$\sigma_{c} = \sigma_{p-c}\left[\frac{\varepsilon}{\varepsilon_{p-c}} \exp\left(1 - \frac{\varepsilon}{\varepsilon_{p-c}}\right)\right]^{c} \tag{10}$$

while σ_{p-c} is peak stress calculated, determined in principle according to of Eq.(7)

ε_{p-c} is peak strain calculated according to of Eq. (8)

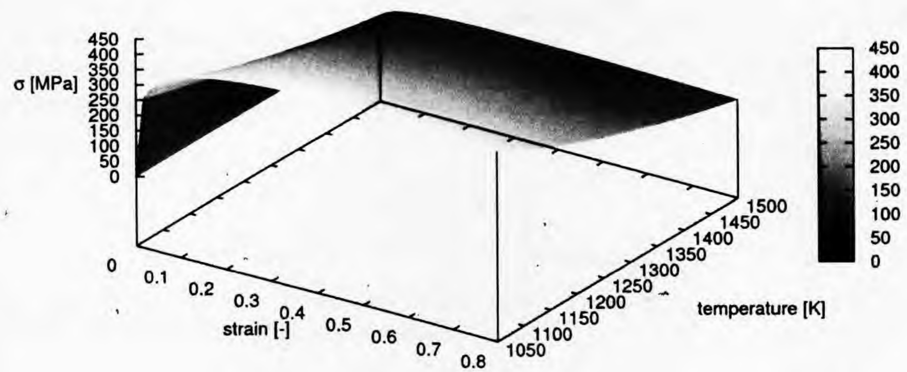

Fig. 1 Stress-strain curves for various temperatures at strain rate at 10 s^{-1}

Based on equation (8) reversed calculations of strain resistance values were performed in Excel and later in gnuplot software in dependence on basic variables. (Low and high levels of strain rate were extrapolated).

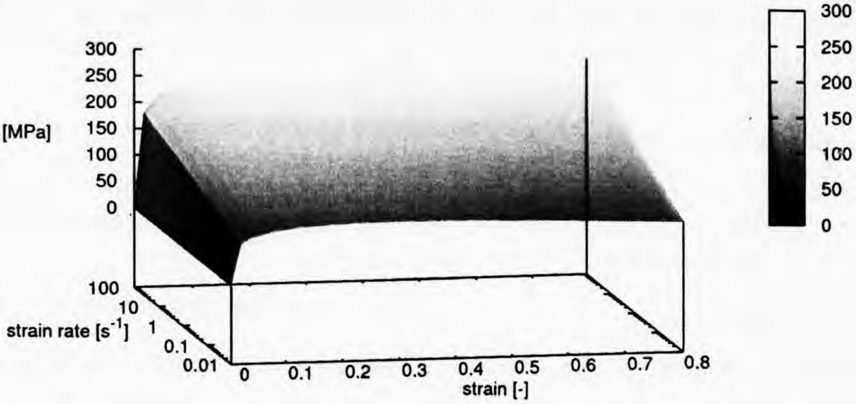

Fig. 2 Stress-strain curves for various strain rates at temperature of 1273 °C

Further procedure is based on specification of individual exponents m, which is determined by regression of dependences. Resulting m in gnuplot software is used for specification of effectiveness according to equation (4). Following graphic illustration, where x and y axes of special graph do not exhibit a regular coordinate network will be carried out by the same gnuplot programme with incorporated procedures. Figure 3. shows resulting surface picture.

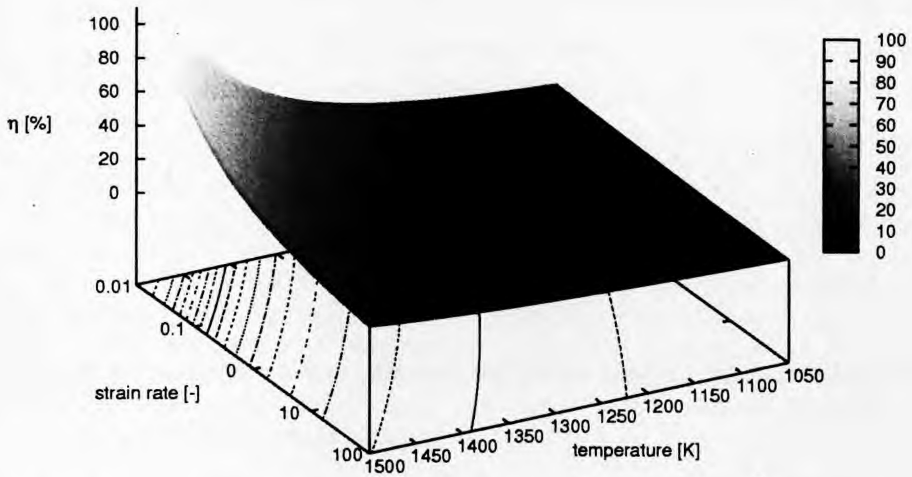

Fig. 3 Surface picture of dissipation energy map (technological maps) for $\varepsilon = 0{,}2$

3. Discussion and conclusion

Physical interpretation of energy dissipation (dissipation maps, processing maps) is based on the assumption that dynamic recovery takes place more intensively at lower temperature and in shorter time than dynamic recrystallization which occurs at typical strain rates and is stable at higher temperatures. The created dissipation maps can reveal domains of maximum efficiency of the processes. However, the maps can also show regions of instability of the hot forming process. Our experimental steel exhibited very uniform flow stress curve and a logical dependence on temperature and strain rate. Hence, a continuous curve of energy dissipation efficiency could be expected, as evidenced by Fig. 3. No instability regions were found. Finding other instability regions would require much wider temperature range, particularly in the lower temperature areas. However, it was not feasible due to plastometric experiments which had been conducted. They were plane strain compression tests (PSCT) performed in Gleeble 3500 which did not include lower temperatures. The optimum parameters thus remain in the region above 950 to 1000 °C with strain rate of 1 s^{-1} and lower. At higher strain rates the process shows lower efficiency.

Acknowledgements

This work was supported by NATIONAL SCIENCE FOUNDATION of the Czech Republic under the project No. GAČR 106/07/063. Experiments were performed under the MSM 6198910015 research plan. Additional support was provided by project FI-IM 5/049.

References

[1]. ALEXANDER, J.M.: in Modelling of Hot Deformation of Steels, (1984), 101.

[2]. GEGEL, H.L. et al.: Metals Handbook, (1987), 417.

[3]. CHANG, T.C.- WANG, J.Y.- O, C.M.- LEE, S.: J. Mater. Proc. Technol., 140, (2003), 588-591.

[4]. LAPOVOK, R.YE.- BARNETT, M.R.- DAVIES, C.H.J.: J. Mater. Proc. Technol., 146, (2004), 408-414.

[5]. JAGER, A.- LUKAC, P.- GARTNEROVA, V.- HALODA, J.- DOPITA, M.: Mater. Sci. Eng., A432, (2006), 20-25.

[6]. PRASAD, Y.V.R.K. et al.: Metall. Transactions, (1984), 1883-92.

[7]. VENUGOPAL, S. et al.: Metall. Transactions, (1992), 3093-03.

[8]. PRASAD, Y.V.R.K.- RAO, K.P.: Materials and Design, 30, (2009), 3723-3730.

[9]. PRASAD, Y.V.R.K.- RAO, K.P.: Materials Science and Engineering, A487, (2008), 316-327.

[10]. MATAYA, M.C. et al.: Metall. Transactions, (1983), 1681-95 a 1669-87.

[11]. KLIBER, J.- SCHINDLER, I.- KUŘE, F.: Tvařitelnost ocelí za tepla, (1989).

[12]. KLIBER, J.- SCHINDLER, I.: Deformation resistance, (1995), 433-5.

[13]. KLIBER, J.: Int. Conference Forming 97, (1997), ISBN 80-7078-466-0, 6.

[14]. KLIBER, J.: Int. Conference Machine-Building and Technosphere at the Boundary of the XXI Century. Doneck, (2001), 144.

Reviewer: Ing. Zdeněk Vašek, Ph.D., Arcelor Mittal Ostrava